Resonant Raman scattering on free and bound excitons in GaN

A. Kaschner,* A. Hoffmann, and C. Thomsen
Institut für Festkörperphysik, Technische Universität Berlin, Hardenbergstr. 36, D-10623 Berlin, Germany
(Received 12 February 2001; published 5 October 2001)

We comprehensively investigated the resonant Raman scattering effect in GaN at low temperatures applying a frequency-doubled titan-sapphire laser as quasicontinuous excitation source. The scattering cross sections of the E_2(high), A_1(LO), and $2A_1$(LO) phonon modes exhibit a resonance enhancement at the donor- and acceptor-bound excitons. The enhancement of the A_1(LO) modes is even stronger than for the nonpolar E_2(high) mode due to a Fröhlich interaction. Furthermore, the temporal behavior of the phonons near the resonance was studied using time-resolved spectroscopy. We found that the resonance process below the bound excitons is likely to proceed via the free exciton as intermediate state.

DOI: 10.1103/PhysRevB.64.165314 PACS number(s): 61.66.−f, 61.72.Ff

I. INTRODUCTION

Resonant Raman scattering (RRS) has been studied for a variety of semiconductor materials, such as CdS,[1] GaP,[2] and GaAs,[3] since the late 1960. In particular, effects of RRS on free and bound excitons in CdS were extensively investigated[4–6] because crystals of high structural quality were synthesized and intentionally doped. In the III-V nitride material system the resonance enhancement of the Raman scattering cross section was used to detect inelastic scattered light from small sample volumes, for instance, in buried AlGaN structures[7] and indium fluctuations in the ternary alloy InGaN.[8–11] There are a few studies on RRS in GaN.[12–16] One of the first RRS experiments on GaN was carried out by Lemos *et al.*[15] For excitation energies from 800 to 300 meV below the band gap, they did observe a resonance enhancement of the A_1(TO), E_1(TO), and E_2(high) modes. In previous experiments a fixed excitation energy and a temperature-variable cryostat are used to match the excitation energy with the resonance. In Ref. 12 temperatures between 300 and 870 K were applied and, therefore, no resonance with bound excitons could be observed. RRS on acceptor-bound excitons in GaN at temperatures of 80 and 130 K was reported in Ref. 14. In the present study we applied a frequency-doubled titan-sapphire laser as quasicontinuous excitation source to investigate RRS in GaN at low temperatures, where bound excitons exist. Furthermore, we studied the temporal behavior of the phonons near the resonance using time-resolved spectroscopy.

II. EXPERIMENT

The sample under study was a not intentionally doped 220-μm-thick GaN film grown by hydride vapor phase epitaxy (HVPE). Sapphire (0001) with a sputtered ZnO buffer layer was used as substrate.[17] The Raman spectra were taken in a quasibackscattering geometry: i.e., the exciting laser beam hit the sample under 45°. Due to the large refractive index of GaN, the propagation direction of the beam in the material deviates only a few degrees from the sample normal. The sample was excited with a frequency-doubled titan-sapphire laser providing excitation wavelength between 352 and 387 nm. The laser was operated in pulsed mode with a repetition rate of 80 MHz. Proper color filters were used to improve the ultraviolet-to-infrared ratio of the exciting beam. The sample was mounted in a cryostat operating at suprafluid helium temperature (1.8 K) or liquid nitrogen temperature (77 K). The signal was detected through a subtractive double-grating monochromator with a UV-enhanced multichannel-plate photomultiplier. For time-resolved measurements the system response to a laser pulse with a full width at half maximum (FWHM) of approximately 30 ps was taken into account for analysis of the transients using deconvolution techniques. For the photoluminescence (PL) measurements the sample was mounted in a He bath cryostat and a HeCd laser was used as excitation source.

III. RESULTS AND DISCUSSION

A. RRS at 1.8 K

Prior to the RRS experiments, we investigated the luminescence properties of a variety of GaN samples in order to select a crystal exhibiting high crystalline quality and both acceptor- and donor-bound excitonic luminescence. Figure 1 shows a PL spectrum of the sample under study. In the inset the region of excitonic luminescence is depicted on a logarithmic scale for clarity. The spectrum is dominated by the

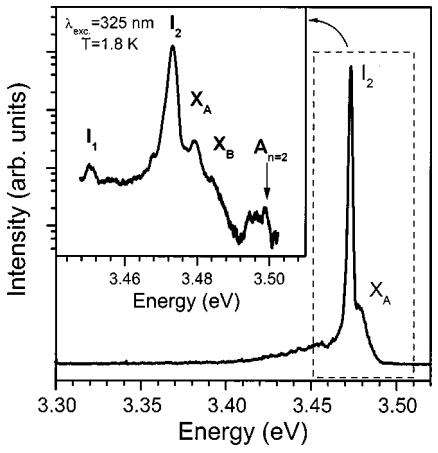

FIG. 1. Photoluminescence spectrum of the investigated sample at 1.8 K. The inset shows the region of the free and bound excitons on a logarithmic scale.

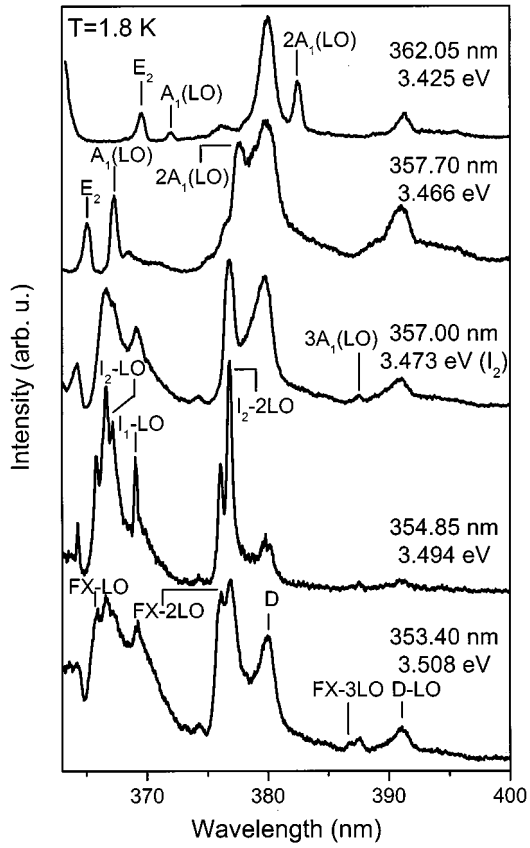

FIG. 2. Spectra at 1.8 K taken for different excitation energies in the vicinity of the donor-bound exciton. Beside the phonon replicas of the free and bound excitons and the phonon modes, a defect luminescence (*D*) can be observed.

luminescence of excitons bound to neutral donors (I_2) at 3.473 eV. On the high-energy side of the I_2, we find the free exciton X_A (3.479 eV) and as a shoulder X_B (3.485 eV).[18] A weak multiple structure peaking at energies of 3.494, 3.497, and 3.499 eV can be assigned to excited states of free and bound excitons according to Ref. 19. In addition to the strong I_2, we also find a weaker luminescence around 3.451 eV originating from recombination of acceptor-bound excitons (I_1). The chemical nature of the acceptor was suggested to be Zn, which can diffuse from the buffer layer at high growth temperatures.[20,21]

Figure 2 shows spectra taken at different excitation energies. The excitation for the two lower spectra is above the energy of the free *A* and *B* excitons (FX). The 1LO and 2LO phonon replicas of the free *A* excitons and the donor- and acceptor-bound excitons are observed. An additional luminescence *D* at 380 nm and its 1 LO replica at 391 nm is apparent (also *D*-2LO can be observed, but is not shown here). From the energetic position one could assign *D* as donor-acceptor pair (DAP) recombination[22,23] or a 2LO replica of I_1. However, the structure does not exhibit the typical DAP line shape with merging LO replicas and a broad FWHM. The interpretation of *D* being the I_1-2LO can be excluded, because of its very long luminescence decay, which does not fit into the 12.5-ns window provided by our

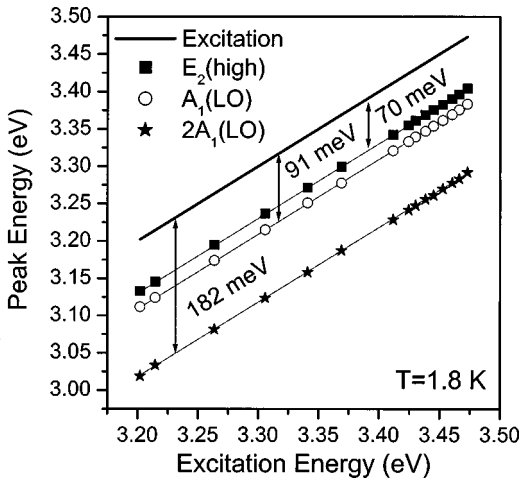

FIG. 3. Peak energy vs excitation energy of the modes appearing in the spectra at 1.8 K. The thick line represents the excitation energy itself, whereas the thin lines are shifted by the energies of the E_2(high) (solid square), A_1(LO) (open circle), and $2A_1$(LO) (star) phonon modes of hexagonal GaN.

system with a repetition rate of 80 MHz. Furthermore, the *D* luminescence can be excited with energies below I_1. We rather think that the origin of *D* is the recombination of excitons, deeply bound, for instance, at dislocations or other defects. We observe up to a three-phonon replica of the *D* luminescence, which indicates a strong coupling to the crystal lattice and is typical for this kind of defects. The excitation wavelength of 357 nm (3.473 eV) is exactly in resonance with the I_2 state. The structures in the corresponding spectrum appear broadened. Here one cannot distinguish between the LO replica of the I_2 and the A_1(LO) phonons generated by the Raman effect, whereas in the two upper spectra of Fig. 2 a clear shift of the mentioned structures is obvious. We observe the E_2(high), A_1(LO), and $2A_1$(LO) phonon modes of GaN—having intensities comparable with the luminescence features—resonantly enhanced using an excitation close to the I_2 energy. A subsequent reduction of the excitation energy leads to a shift of the phonon lines parallel to the exciting laser line with an energetic difference corresponding to the E_2(high), A_1(LO), and $2A_1$(LO) energy (Fig. 3). Within the experimental accuracy of our experiment, the shift of $2A_1$(LO) line equals a value of twice the shift of the A_1(LO) line. In previous experiments[10] we found that actually the relation $\omega_{2LO} < 2\omega_{1LO}$ holds. For multiphonon processes the phonons are no longer restricted to the center of the Brillouin zone and, therefore, the frequency of the $2A_1$(LO) band is slightly lower than the A_1(LO) frequency multiplied by 2.

In Fig. 4(a) the normalized intensities of the A_1(LO) and $2A_1$(LO) mode are depicted as function of the exciting wavelength. We have chosen the intensity of the *D* luminescence to normalize the phonon intensities for comparability reasons. One has to be aware that *D* itself has an excitation behavior, which influences the intensity ratio with shifting the excitation wavelength towards 380 nm. Both the A_1(LO) and $2A_1$(LO) phonon modes show a significant resonance behavior when the excitation energy approaches the I_1 and

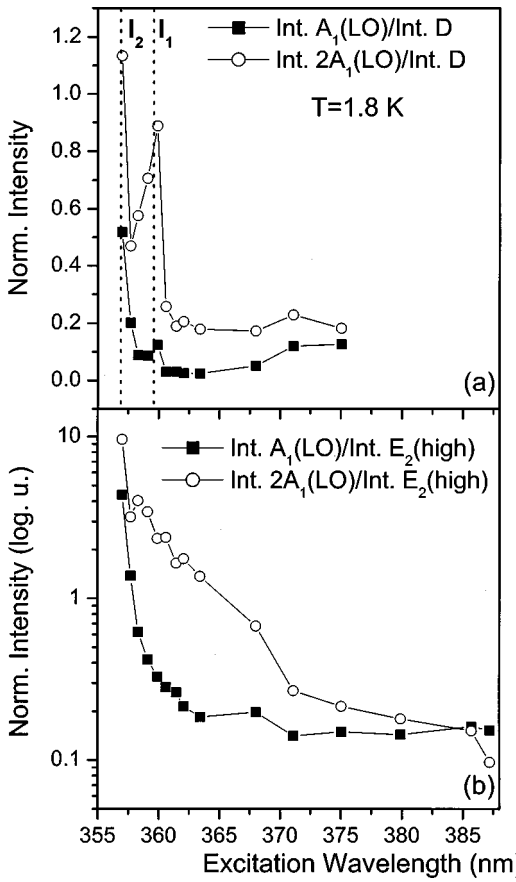

FIG. 4. Intensity of the $A_1(\mathrm{LO})$ and $2A_1(\mathrm{LO})$ mode normalized on the intensity of the defect luminescence D (a) and $E_2(\mathrm{high})$ phonon mode (b) vs excitation energy at 1.8 K. Lines are a guide to the eye only.

I_2, respectively. The bound excitation resonances superimpose a background which continuously increases with decreasing wavelength. As described for CdS,[4] this background is presumably due to the free-exciton contribution.

We also find the $E_2(\mathrm{high})$ phonon mode appearing resonantly enhanced in the spectra. An antiresonance behavior like for the $E_2(\mathrm{low})$ in CdS (Ref. 5) is not observed. Normalizing the $A_1(\mathrm{LO})$ mode intensities to the $E_2(\mathrm{high})$ intensity yields a different picture [Fig. 4(b)]. Tuning the excitation from 390 to 357 nm results in a by two orders of magnitude increased $A_1(\mathrm{LO})/E_2(\mathrm{high})$ ratio (compare with Refs. 12 and 16). The $E_2(\mathrm{high})$ mode is also resonantly enhanced in the vicinity of the bound excitons, because of the vanishing denominator in the Raman scattering cross section. However, the $E_2(\mathrm{high})$ mode is nonpolar and does not interact via Fröhlich interaction as the LO modes do. Therefore, in Fig. 4(b) we only see the polar portion of the resonance process. The probability to generate a real electron-hole pair as intermediate state in the Raman process decreases with the energetic distance from the band gap. As a result, this has a large effect on the scattering intensities.

It seems to be a general effect that the $2A_1(\mathrm{LO})$ scattering intensity is larger than the $A_1(\mathrm{LO})$ intensity in the vicinity of excitonic resonances.[10,12,14] At first sight this is surprising since a nonresonant second-order process is usually by orders of magnitude less probable than a first-order Raman process. For our sample the $A_1(\mathrm{LO})/2A_1(\mathrm{LO})$ intensity ratio is smaller than unity in the energy region between 3.25 and 3.50 eV (Fig. 5). A possible explanation for the behavior between 3.40 and 3.50 eV can be given within the polariton model according to Refs. 24 and 25. The $A_1(\mathrm{LO})$ scattering is proportional to the square of the wave vector of the created phonon. When the energy of the excited polaritons is increased, their wave vectors increase, leading to a higher $A_1(\mathrm{LO})$ scattering intensity, whereas the $2A_1(\mathrm{LO})$ process does not depend on the polariton wave vector. This argumentation qualitatively explains the increasing $A_1(\mathrm{LO})/2A_1(\mathrm{LO})$ intensity ratio between 3.40 and 3.50 eV (compare with Fig. 2 in Ref. 24). The increase in the $A_1(\mathrm{LO})/2A_1(\mathrm{LO})$ intensity ratio for decreasing energies between 3.40 and 3.20 eV is just a result of the increasing energetic difference to the excitonic resonance: i.e., the intensity ratio converges towards the value for the nonresonant case where $A_1(\mathrm{LO})$ is dominant. It is expected that in principle the behavior is similar for all GaN samples. However, the absolute values for the $A_1(\mathrm{LO})/2A_1(\mathrm{LO})$ intensity ratio depends, for instance, on the free-carrier concentration, doping,[26] and structural quality of the sample. We found for a variety of samples a relative increase of the $2A_1(\mathrm{LO})$ mode with increasing structural quality.

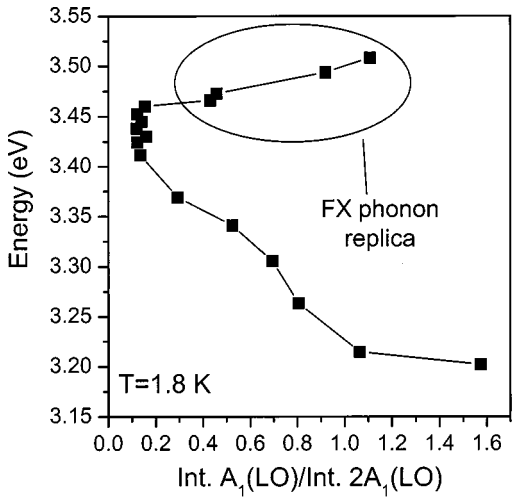

FIG. 5. Intensity ratio of the $A_1(\mathrm{LO})$ and $2A_1(\mathrm{LO})$ phonon mode as a function of energy. For a better comparability with Fig. 2 of Ref. 24, the intensity and energy axes are exchanged. Note that the data points in the ellipse are determined by the respective FX phonon replica, since the corresponding phonon modes are not observed at these excitation energies.

B. RRS at 77 K

Most of the donor-bound excitons are dissociated at 77 K due to the I_2 binding energy of approximately 6 meV. Since the acceptor binding energy is considerably larger than the donor binding energy, the acceptor-bound excitons are just marginally dissociated. Resonant Raman scattering at acceptor-bound excitons can be studied exclusively at 77 K without superposition of the effect of the donor-bound exci-

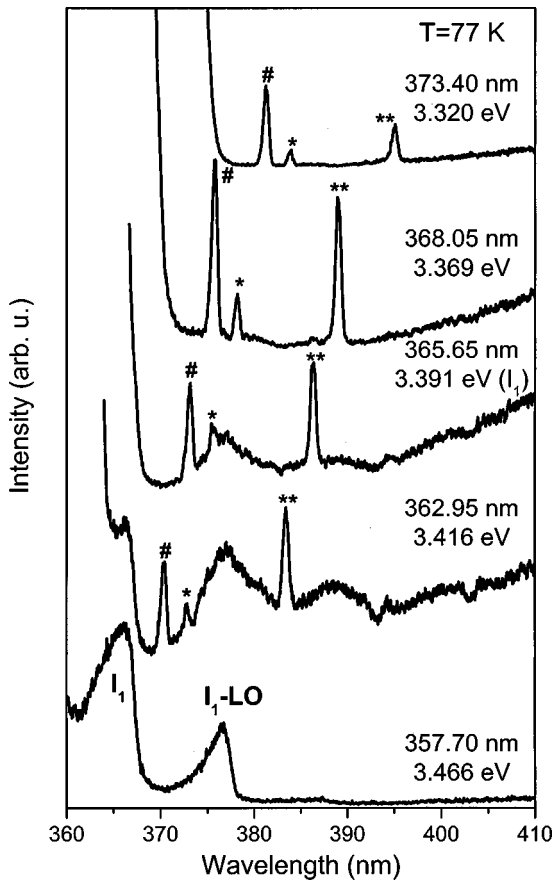

FIG. 6. Spectra at 77 K taken for different excitation energies in the vicinity of the acceptor-bound exciton. The symbols mark the E_2(high) (#), A_1(LO) (*), and $2A_1$(LO) (**) modes.

tons whose density is much higher at 1.8 K. Figure 6 shows various spectra taken at 77 K using different excitation energies. In the lowest spectrum the acceptor-bound exciton and the corresponding 1LO replica can be seen. In addition to these broad structures, three very narrow lines appear at an excitation energy of 3.416 eV (362.95 nm). Whereas the I_1 and I_1-LO vanish at even lower excitation energies, the three narrow lines still appear in the spectra. The peak positions of these three lines are represented in a similar figure (Fig. 7) then for the 1.8-K case (Fig. 3). From Fig. 7 it is obvious that the sharp lines in the spectra of Fig. 6 correspond to the E_2(high), A_1(LO), and $2A_1$(LO) Raman modes of hexagonal GaN.

The results of the 77-K measurements are sketched in a resonance profile (Fig. 8). Here the intensity of the $2A_1$(LO) mode was normalized to that of the E_2(high) mode. As discussed above, one can distinguish between the polar versus nonpolar scattering mechanisms with this method. However, no other feature present in all spectra could be used for normalization. We find an astonishingly good agreement of the I_1 luminescence maximum with that of the Raman resonance profile, which evidences the I_1 states to be the real intermediate energy levels for the resonant Raman process. Tuning the excitation energy to lower energies (larger wavelength) results in a decrease in Raman scattering efficiency, but at 379.1 nm all three Raman modes are still observable. Raman

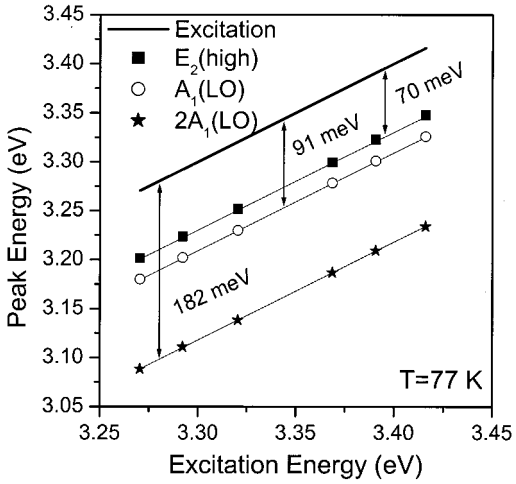

FIG. 7. The peak energy vs excitation energy of the modes appearing in the spectra at 77 K is depicted. The thick line represents the excitation energy itself, whereas the thin lines are shifted by the energies of the E_2(high), A_1(LO), and $2A_1$(LO) phonon modes of hexagonal GaN.

scattering in resonance with acceptor-bound excitons was previously reported for a similar GaN sample.[14] In distinction to the previous measurements, where the band gap was tuned by temperature variation and a fixed laser energy was used, the present experiment gives direct evidence for the resonance process with acceptor-bound excitons using different excitation energies at a fixed temperature.

Comparing the results from Secs. III A and III B, we find a resonance enhancement of the Raman scattering effect when the energy of the incoming photon matches the energy of acceptor- and donor-bound excitons, respectively. The Raman modes are not observed when the excitation energy is slightly above the bound exciton energy. In this case only phonon replicas of the bound excitons are present in the

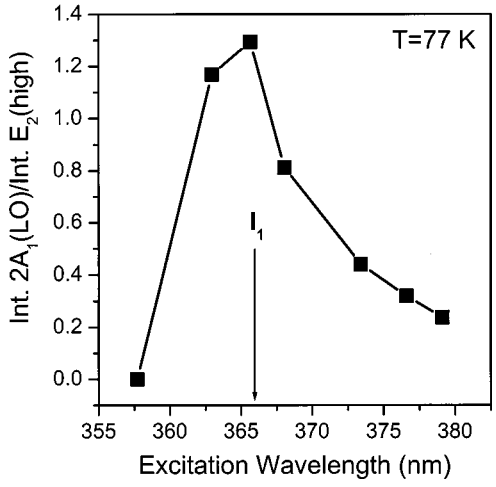

FIG. 8. Intensity of the $2A_1$(LO) mode normalized on the intensity of the E_2(high) phonon mode vs excitation energy (77 K). A maximum appears at the energetic position of the I_1 line. Lines are a guide to the eye only.

spectra. This is different to the case of CdS, where both phonon replica and resonantly enhanced phonon modes are observable at the same time under such excitation conditions.[4,27] Within the polariton model, which has to be applied in the case of a strong exciton-light interaction, both processes are very similar and can be described as polariton scattering with phonons. If the initial state of the scattered polariton is purely excitonic, then the inelastic scattering can be regarded as a LO replica of the excitonic luminescence. If the initial state is purely light, Raman scattering is observed.

C. Time-resolved Raman and luminescence experiments

There are few publications on phonon lifetimes in GaN. Siegle *et al.*[28] used time-resolved anti-Stokes Raman scattering and determined an upper limit for the decay time of nonequlibrium LO phonons in GaN to 4 ps. Bergman *et al.*[29] evaluated phonon lifetimes in GaN via the energy-time uncertainty measuring the Raman linewidth. Except for the E_2(low) mode, they found phonon lifetimes shorter than 1 ps. The homogeneous linewidth is mainly determined by impurity scattering and crystal anharmonicity. It was suggested that LO phonons in GaN decay into TO and LA phonons to explain the short phonon lifetimes, because a decay into two LA phonons is unlikely due to energetic considerations.[30] In the present work we investigate the decay times of phonons and phonon replicas under excitation conditions close to excitonic resonances by means of time-resolved spectroscopy.

For the excitonic luminescence processes, we obtain decay times of 90 ps (FX), 270 ps (I_2), and 440 ps (I_1) within an experimental accuracy of $\pm 10\%$. It is noteworthy that the I_2 (I_1) onset time matches the FX (I_2) decay time, which suggests corresponding transfer processes (Fig. 9). Compared with previously published values,[16,31,32] these are surprisingly long decay times, especially for the FX and I_2. Only Harris *et al.*[33] reported a FX decay time of 125 ps for high-quality HVPE GaN. The sample used in our experiment is also of good crystalline quality, having a low defect density. Also, the fact may contribute that the sample is irradiated by a small portion of the not frequency-doubled infrared laser light in addition to the actual exciting wavelength in spite of using a color filter. The energy of the infrared light is sufficient to fill deep defect levels and, thus, can block nonradiative recombination channels. Hence the decay time draws nearer to the real radiative lifetime.

Figure 10 shows the transition in the temporal behavior from the I_2 phonon replica to the A_1(LO) phonon mode. The secondary peaks appearing for some of the transients are measurement artifacts and do not affect the decay times determined by the deconvolution procedure. Exciting above I_2, we obtain decay times of more than 200 ps for the I_2-1LO corresponding to the I_2 decay time. For excitation energies below the I_2 energy, only the resonantly enhanced phonon modes are present in the spectra. The decay is dominated by a fast component. The transients look similar to the system response to a laser pulse, and deconvolution yields decay times of a few ps, which is less than the accuracy of this experiment. If the excitation energy matches exactly the I_2 energy (357.00 nm), the transient appears to be composed of a fast and a slow component. In this case one cannot distinguish between the phonon replica of the luminescence and the phonon mode as from its energetic position. The structure in the spectrum consists of both of these processes. To the best of our knowledge this is the first direct observation of the change in the temporal behavior during the continuous transition from the phonon replica of excitonic luminescence to the phonon modes.

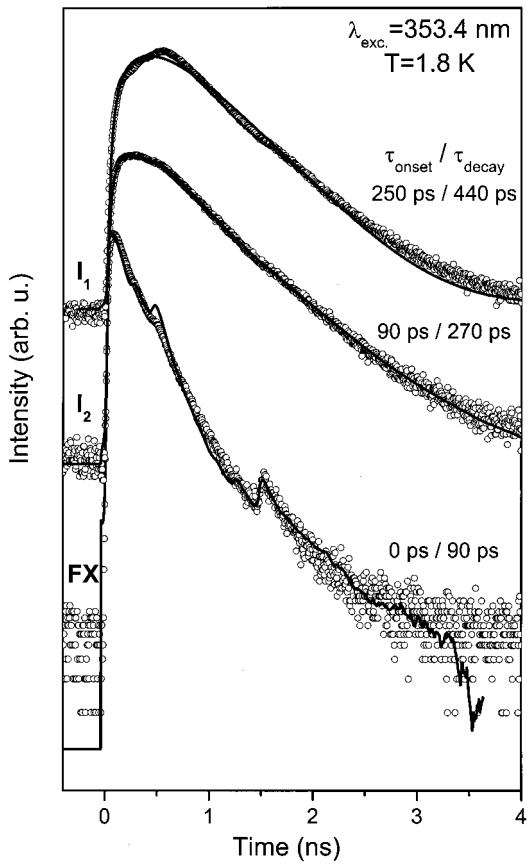

FIG. 9. Transients (open circles) of the free and bound excitons on logarithmic scale taken at 1.8 K under excitation with 353.4 nm and the corresponding fit (lines).

Another proposition of our work was to check the following idea. The intermediate exciton state in a resonant Raman process is real and not virtual as for off-resonant excitation conditions. Therefore, one can suppose that the time between the exciting laser pulse and the emission of the scattered photon is determined by the lifetime of the exciton involved.

Beside the very fast component, i.e., a few ps as reported in Refs. 28 and 29, the transients of the phonon modes consist of a second component decaying with τ_2. The decay time τ_2 versus excitation wavelength is depicted in Fig. 11. The very long τ_2 times of more than 600 ps at excitation wavelengths of 357.70 and 358.30 nm originate from a luminescence structure superimposing the A_1(LO) mode. Between 359.10 and 363.40 nm the τ_2 value is close to the I_2 decay time. An interesting feature appears for wavelengths larger than 368.00 nm. The slow decay constant varies in the range from 60 to 110 ps with an amplitude ratio τ_2/τ_1 of 1/20. Remarkably, these values agree with the FX decay time

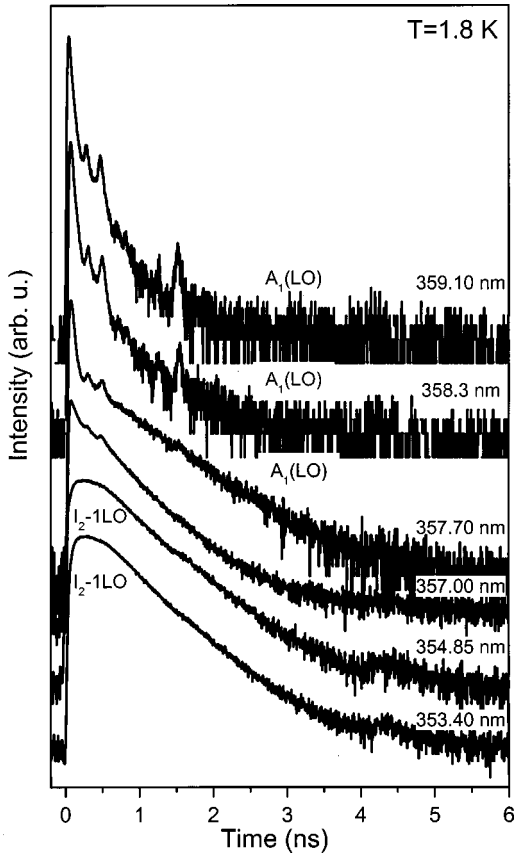

FIG. 10. Transients of the LO phonon replica of I_2 and the A_1(LO) phonon mode, respectively, taken for various excitation energies. A drastic change in the decay behavior is obvious during the transition.

within the experimental accuracy. It should be mentioned that the E_2(high) and $2A_1$(LO) mode show a similar behavior. There is no other luminescence energetically superimposing the phonon modes in these cases. Thus we found evidence from the temporal behavior of the phonon modes that the resonance process for excitation below the bound excitons proceeds via the free exciton as intermediate state. The portion of τ_2 is small, because the electron-phonon interaction proceeds on a time scale which is short compared to the FX decay time. Hence the decay of resonantly excited phonons is mainly determined by the fast component τ_1, but still there is a certain fraction in the transients reflecting the excitonic lifetime.

IV. SUMMARY

We found experimental evidence for resonance Raman scattering in GaN with donor- and acceptor-bound excitons. The E_2(high), A_1(LO), and $2A_1$(LO) Raman modes are resonantly enhanced when the energy of the incoming photon matches the bound exciton energy or is slightly below. Whereas the polar LO modes are also subject to the Fröhlich interaction, the nonpolar E_2(high) mode interacts only via deformation-potential interaction. This is reflected in the LO/E_2(high) ratio, which increases towards the excitonic resonances. At 77 K, where most of the donor-bound excitons are dissociated, we continue to observe a strong resonance with the acceptor-bound excitons nicely confirming the results in Ref. 14. We suggest Zn diffusion from the buffer layer in the GaN film to be the chemical origin of the acceptor states.

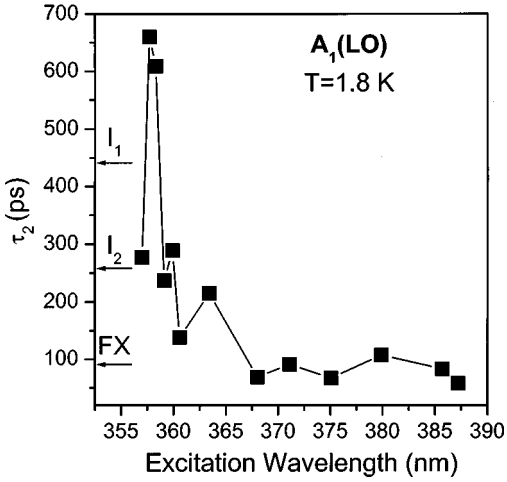

FIG. 11. Slow decay constant (τ_2) of the A_1(LO) phonon decay as function of the excitation wavelength. The arrows indicate the decay times of free and bound excitons. Lines are a guide to eye only.

Furthermore, we investigated the change in the decay behavior during the transition from phonon replicas to resonantly enhanced phonon modes. As expected, the phonon replicas exhibit the same decay constant as the bound exciton, whereas the decay of the phonons is dominated by a fast component, which is only a few ps, i.e., below the accuracy of this experiment. However, we found a larger decay constant with a lower amplitude in the decay characteristic for all phonons. For excitation conditions below the bound excitons, this second decay time is close to the measured free-exciton decay constant. We suggest that the free exciton is the intermediate state for the resonance process in this region.

ACKNOWLEDGMENTS

A.K. would like to acknowledge an Ernst van Siemens-Scholarship. Part of this work was supported by Deutsche Forschungsgemeinschaft. The authors would like to thank Professor K. Hiramatsu (Mie University) for providing the high-quality GaN sample.

*Corresponding author. Electronic address: kaschner@physik.tu-berlin.de

[1] R. C. C. Leite, J. F. Scott, and T. C. Damen, Phys. Rev. Lett. **22**, 780 (1969).
[2] B. A. Weinstein and M. Cardona, Phys. Rev. B **8**, 2795 (1973).
[3] R. Trommer and M. Cardona, Phys. Rev. B **17**, 1865 (1978).
[4] T. C. Damen and J. Shah, Phys. Rev. Lett. **27**, 1506 (1971).
[5] T. C. Damen and J. F. Scott, Solid State Commun. **9**, 383 (1971).

[6] R. Baumert, I. Broser, J. Gutowski, and A. Hoffmann, Phys. Status Solidi B **116**, 261 (1983).
[7] M. Yoshikawa, J. Wagner, H. Obloh, M. Kunzer, and M. Maier, J. Appl. Phys. **87**, 2853 (2000).
[8] D. Behr, J. Wagner, A. Ramakrishnan, H. Obloh, and K.-H. Bachem, Appl. Phys. Lett. **73**, 241 (1998).
[9] N. Wieser, O. Ambacher, H.-P. Felsl, L. Görgens, and M. Stutzmann, Appl. Phys. Lett. **74**, 3981 (1999).
[10] A. Kaschner, A. Hoffmann, C. Thomsen, T. Böttcher, S. Einfeldt, and D. Hommel, Phys. Status Solidi A **174**, R4 (2000).
[11] V. Lemos, E. Silveira, J. R. Leite, A. Tabata, R. Trentin, L. M. R. Scolfaro, T. Frey, D. J. As, D. Schikora, and K. Lischka, Phys. Rev. Lett. **84**, 3666 (2000).
[12] D. Behr, J. Wagner, J. Schneider, H. Amano, and I. Akasaki, Appl. Phys. Lett. **68**, 2404 (1996).
[13] D. J. Dewsnip, A. V. Adrianov, I. Harrison, D. E. Lacklison, J. W. Orton, J. Morgan, G. B. Ren, T. S. Cheng, S. E. Hooper, and C. T. Foxon, Semicond. Sci. Technol. **12**, 55 (1997).
[14] A. Kaschner, A. Hoffmann, and C. Thomsen, Phys. Status Solidi B **223**, R11 (2001).
[15] V. Lemos, C. A. Arguello, and R. C. C. Leite, Solid State Commun. **11**, 1351 (1972).
[16] S. Tripathy, R. K. Sony, H. Asahi, K. Iwata, R. Kuroiwa, K. Asami, and S. Gonda, J. Appl. Phys. **85**, 8386 (1999).
[17] T. Detchprohm, K. Hiramatsu, H. Amano, and I. Akasaki, Appl. Phys. Lett. **61**, 2688 (1992).
[18] D. Volm, K. Oettinger, T. Streibl, D. Kovalev, M. Ben-Chorin, J. Diener, B. K. Meyer, J. Majewski, L. Eckey, A. Hoffmann, H. Amano, I. Akasaki, K. Hiramatsu, and T. Detchprohm, Phys. Rev. B **53**, 16 543 (1996).
[19] B. J. Skromme, J. Jayapalan, R. P. Vaudo, and V. M. Phanse, Appl. Phys. Lett. **74**, 2358 (1999).
[20] A. Hoffmann, J. Holst, A. Kaschner, H. Siegle, J. Christen, P. Fischer, F. Bertram, and K. Hiramatsu, Mater. Sci. Eng., B **59**, 163 (1999).
[21] H. Amano, K. Hiramatsu, and I. Akasaki, Jpn. J. Appl. Phys., Part 2 **27**, L1384 (1988).
[22] S. Fischer, C. Wetzel, E. E. Haller, and B. K. Meyer, Appl. Phys. Lett. **67**, 1298 (1995).
[23] H. Teisseyre, T. Suski, P. Perlin, I. Grzegory, M. Leszczynski, M. Bockowski, S. Porowski, J. A. Freitas, R. L. Henry, A. E. Wickenden, and D. D. Koleske, Phys. Rev. B **62**, 10 151 (2000).
[24] E. F. Gross, S. A. Permogorov, V. V. Travnikov, and A. V. Sel'kin, Sov. Phys. Solid State **13**, 578 (1971).
[25] S. A. Permogorov and V. V. Travnikov, Sov. Phys. Solid State **13**, 586 (1971).
[26] N. Wieser, M. Klose, R. Dassow, F. Scholz, and J. Off, J. Cryst. Growth **189/190**, 661 (1998).
[27] J. F. Scott, R. C. C. Leite, and T. C. Damen, Phys. Rev. **188**, 1285 (1969).
[28] H. Siegle, V. Kutzer, A. Hoffmann, and C. Thomsen, in *Proceedings of the 23rd International Conference on the Physics of Semiconductors*, Berlin, Germany, 1996, edited by M. Scheffler and R. Zimmermann (World Scientific, Singapore, 1996), p. 533.
[29] L. Bergman, D. Alexson, P. L. Murphy, R. J. Nemanich, M. Dutta, M. A. Stroscio, C. Balkas, H. Shin, and R. F. Davis, Phys. Rev. B **59**, 12 977 (1999).
[30] B. K. Ridley, J. Phys.: Condens. Matter **8**, L511 (1996).
[31] L. Eckey, J.-Ch. Holst, P. Maxim, R. Heitz, A. Hoffmann, I. Broser, B. K. Meyer, C. Wetzel, E. N. Mokhov, and P. G. Baranov, Appl. Phys. Lett. **68**, 415 (1996).
[32] R. A. Mair, J. Li, S. K. Duan, J. Y. Lin, and H. X. Jiang, Appl. Phys. Lett. **74**, 513 (1999).
[33] C. I. Harris, B. Monemar, H. Amano, and I. Akasaki, Appl. Phys. Lett. **67**, 840 (1995).